ARCHAEOLOGICAL SIGNATURES IN ARID REGIONS DETECTED BY HIGH-RESOLUTION SATELLITE IMAGES

by Paolo Trivero, Diego Baratono, Maria Borasi, Marco Cavagnero

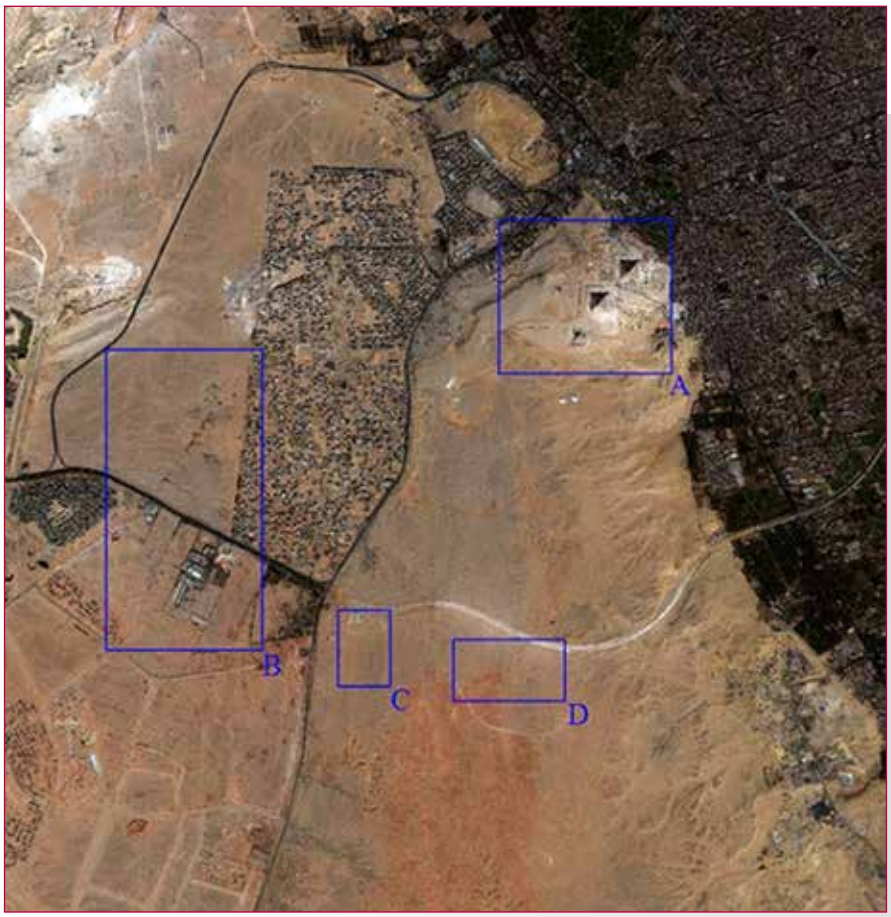

Fig. 1 - GeoEye-1 (25 Mar 2009): study areas of interest A-D (A: Giza Plateau; B: western plateau; C: necropolis; D: ground signs).

A methodology for analyzing very high-resolution (VHR) satellite images has been developed to identify traces of buried structures in arid areas using optical and infrared bands. Applied to the desert north of the Giza plateau, the methodology identified four areas of interest covered by sand. Evidence of mining activity and an underground chamber were found to the west of the pyramids; shadow analysis suggests the presence of buried boats, likely related to the construction of the site. 3D topographic analysis also revealed a probable ancient waterway. Other structures have been discovered that can be traced back to tombs or architectural remains.

The study presents a methodology for analyzing very high-resolution satellite images, applied to the desert north of the Giza plateau. The approach, based on optical and infrared bands and 3D topographic models, has identified traces of quarries, underground cavities, possible boat deposits, and ancient waterways, as well as other archaeological evidence.

The aim of this study is to develop a methodology for analysing Very High Resolution (VHR) satellite imagery in order to detect, locate, and map archaeological features in arid environments. The increasing availability of high-resolution images, acquired under different lighting and viewing conditions, offers new opportunities for accurate landscape analysis (Lasaponara & Masini 2007; Rowlands & Sarris 2007; Trier et al. 2009).

Since the launch of Ikonos in 1999, followed by QuickBird, GeoEye and WorldView, VHR satellites have provided panchromatic data at sub-meter resolution and multispectral bands between 2-4 m. These capabilities, superior to aerial photographs in both spectral range and coverage, have proven particularly effective in arid regions where vegetation marks are absent but traces of microrelief and soil anomalies remain visible (Jahjah & Ulivieri 2010; Traviglia & Cottica 2011).

Numerous studies have confirmed the usefulness of VHR imagery in archaeology, exploiting vegetation indices, spectral signatures, or direct visual interpretation of shapes, dimensions, and shadows (Masini & Lasaponara 2007; Lasaponara & Masini 2007). Automatic and semi-automatic extraction methods have also been applied to identify objects of specific size and geometry (Rowlands & Sarris 2007; Trier et al. 2009).

Within this framework, the Giza Plateau represents both a challenge and an opportunity: its sandy surfaces, long human activity, and monumental setting make it difficult to interpret but highly significant. In this paper we apply a combined approach, including optical and infrared band analysis, multitemporal imagery, shadow-based profiling, dimensional measurements, and 3D topographic modelling, to VHR satellite data of the area, with the aim of detecting anomalies concealed beneath the sand and contributing to the reconstruction of the ancient landscape.

STUDY AREA

We analysed an area of about 100 km² of the Egyptian desert including the site of Giza and its surroundings (Fig. 1).

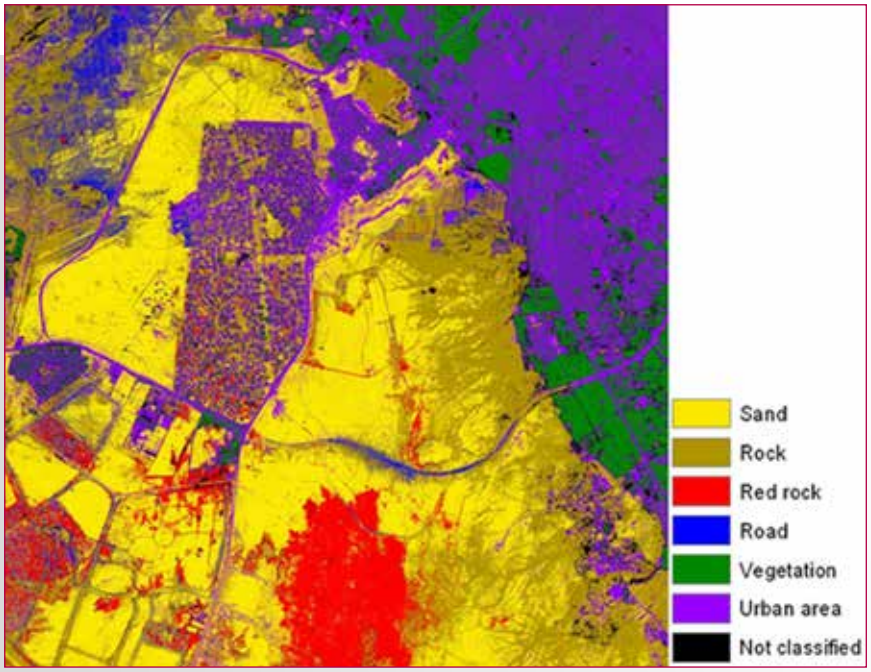

Fig. 2 - Land-cover map of the study area derived from GeoEye-1 imagery.

After visual inspection of high-resolution colour images, displayed both in true colour (R: band 3; G: band 2; B: band 1) and false colour (R: band 4; G: band 3; B: band 2), we identified four areas of interest, outlined in blue in Fig. 1: area A, the Giza Plateau; area B, the western plateau, where 56 tracks possibly represent buried boats, area C (~27 m²) with 975 rectangular *marks suggestive of a workers' village or a necropolis*, and area D with two sand-

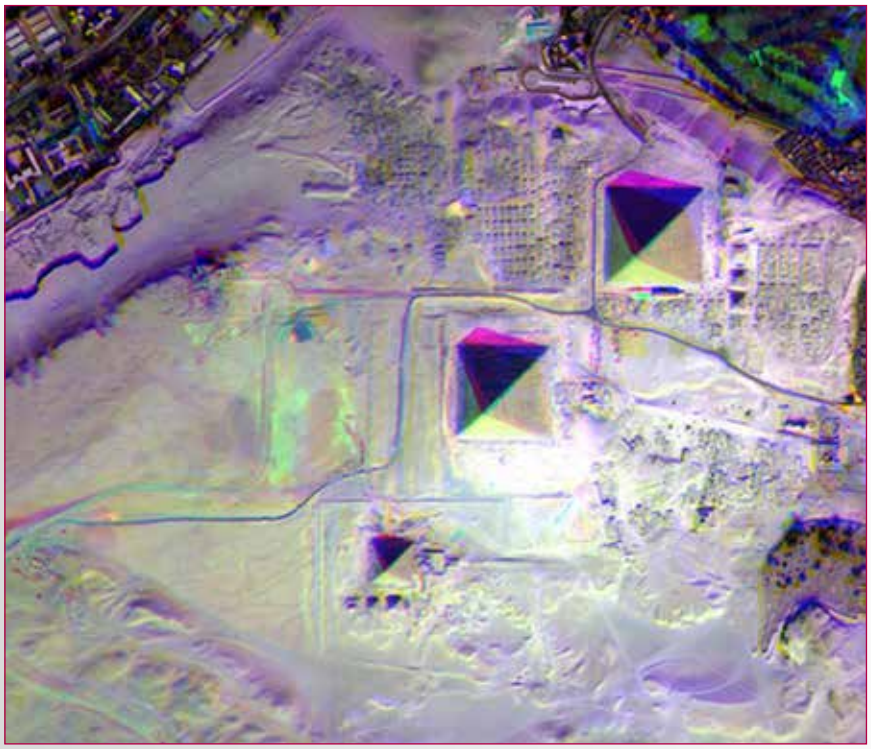

Fig. 3 - Multitemporal RGB image (R = pan 25/03/09; G = pan 05/02/10; B = pan 24/06/11) of Area A (Giza Plateau, see Fig. 1).

Fig. 4 - Multitemporal RGB image (R = pan 25/03/09; G = pan 05/02/10; B = pan 24/06/11) of Area B (see Fig. 1): a) northern sector; b) southern sector.

covered structures resembling a building and 24 U-shaped tracks arranged like towers of a fort.
The land-cover map of the study area from maximum likelihood classification is shown in Fig. 2. The classifier, implemented in ENVI (ITT Visual Information Solutions 2009), assumes normally distributed statistics for each class and assigns each pixel to the class with the highest probability. We selected six training classes (sand, rock, red rock, road, vegetation, urban areas) with a probability threshold of 95%. Results show: sand 31 km^2, rock 24 km^2, red rock 7 km^2, road 4 km^2, vegetation 9 km^2, urban 20 km^2, and 5 km^2 unclassified. All areas of interest fall within the sand class.
To distinguish ancient from recent traces (e.g. car tracks), we created multitemporal images combining panchromatic data from 25/03/09 (red), 05/11/10 (green), and 24/06/11 (blue). Additive combinations highlight temporal variations: equal red+green = yellow; green+blue = cyan; red+blue = magenta; all equal = white. This method, applied to the four areas of interest, produced the multitemporal RGB images shown in Figures 3-6.
Giza is one of the most important archaeological centres of ancient Egypt, hosting the funerary complexes of Khufu, Khafre and Menkaure together with the Sphinx, symbol of divine kingship. Geomorphological studies, field surveys and satel-

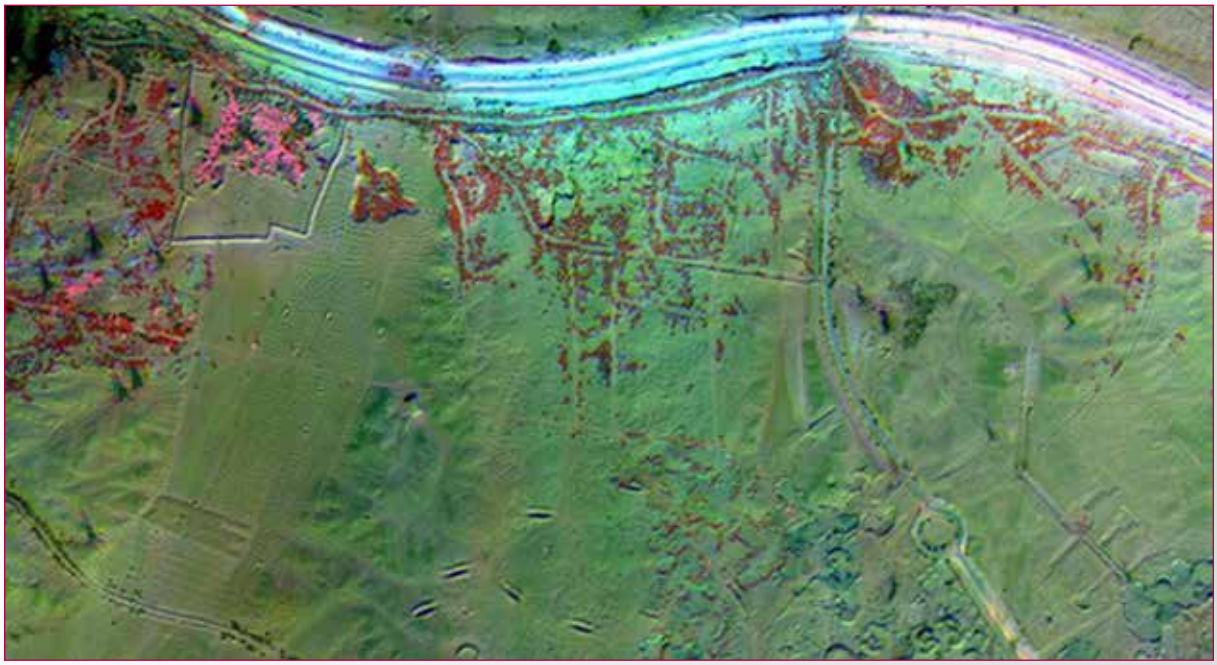

Fig. 5 - Multitemporal RGB image (R = pan 25/03/09; G = pan 05/11/10; B = pan 24/06/11) of Area C (see Fig. 1).

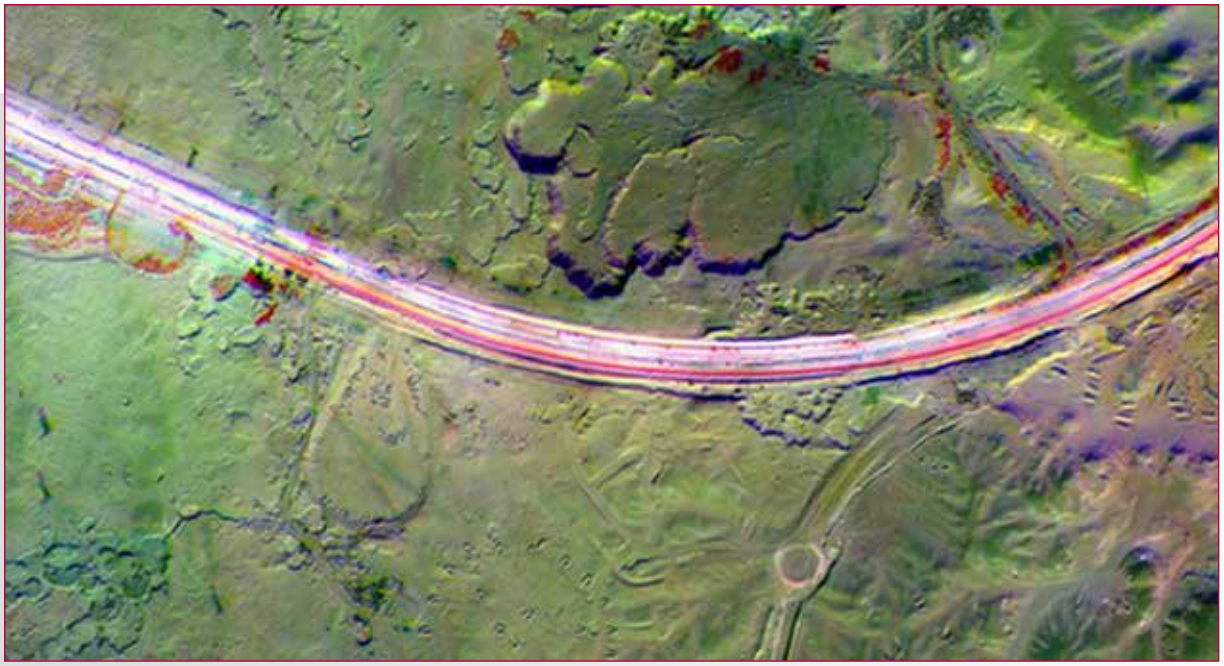

Fig. 6 - Multitemporal RGB image (R = pan 25/03/09; G = pan 05/11/10; B = pan 24/06/11) of Area D (see Fig. 1).

lite analyses (Lutley & Bunbury 2008) show that the Nile shifted laterally over millennia, shaping the distribution of settlements and temples. During the Old Kingdom, the region was crossed by the Ahramat Branch, a secondary Nile channel along the western floodplain, which migrated eastward by more than 2 km per millennium, with particularly marked displacement at Giza.

The elevated causeways of the pyramids ended at an inlet or basin connected to this branch, suggesting their use as ceremonial quays for transporting stone and labour. The Pyramid of Khufu appears to have been built directly on its bank, confirming that the watercourse was active and navigable during the Fourth Dynasty. This proximity offered great logistical advantages, facilitating the movement of materials and workers and influencing the location of the royal funerary complexes.

The later eastward shift of the branch explains why the plateau now appears arid and distant from the Nile. In antiquity, however, Giza occupied a strategic and symbolic position along a vital waterway, significant both practically and ideologically as an expression of royal power. Today the necropolis stands on a rocky plateau ~60 m above sea level, 12 km southwest of Cairo and 7.5–8 km west of the present river.

Khufu's pyramid, the largest, contains about 2.58 million m^3 of stone in 203 courses, with a base of 230.38 m (≈ 440 Royal

Fig. 7 - Portion of GeoEye-1 satellite image of the Giza Plateau. H indicates the heliport.

Fig. 8 - Planimetry with contour lines (m) of the Giza Plateau overlaid on the GeoEye-1 imagery; locations of the presumed and known quarries (A, B, C).

Acquisition date	2009-03-25	2010-11-05	2011-06-24
Acquisition time (GMT)	08:41:11	08:33:19	08:49:01
Cloud cover	0%	0%	0%
Scan Azimuth	98.58°	359.35°	270.81°
Scan Direction	Forward	Reverse	Reverse
Pan Cross Scan*	0.45	0.51	0.47
Pan Azimuth Scan*	0.44	0.50	0.47
MS Cross Scan*	1.80	2.04	1.89
MS Azimuth Scan*	1.77	2.02	1.87
Pan pixel	0.5 m	0.5 m	0.5 m
MS pixel	2 m	2 m	2 m
Nominal collection Azimuth	31.5207°	43.8216°	227.5332°
Nominal collection Elevation	72.37857°	65.91544°	59.79048°
Sun angle Azimuth	142.0453°	158.6482°	109.0889°
Sun angle Elevation	56.10641°	41.66399°	73.34304°

Tab. 1 - Characteristics of the GeoEye-1 dataset
*GMT stands for Greenwich Mean Time. *The data are the acquired nominal GSD*

Radiometric calibration gain *(mW/cm²/μm/sr)*	2009-03-25	2010-11-05	2011-06-24
Panchromatic	0.037260	0.017786	0.017786
Blue	0.055102	0.025017	0.014865
Green	0.038363	0.017183	0.017183
Red	0.060694	0.027738	0.016194
NIR	0.020559	0.009593	0.009593

Tab. 2 - Radiometric calibration gain coefficients (mW/cm²/μm/sr) for the three GeoEye-1 images

Cubits) and an original height of 146.61 m (≈ 280 Royal Cubits), now 138.8 m. Its four faces have an inclination of ~51.8°, and the structure is aligned with the cardinal points. Khafre's pyramid is slightly smaller, with a base of 210.5 m (≈ 402 Royal Cubits) and an original height of 144 m (≈ 275 Royal Cubits). Menkaure's pyramid, the most modest, has a base of 108 m (≈ 206 Royal Cubits) and an original height of 66 m (≈ 126 Royal Cubits).

Fine Tura limestone was used for the outer casing, with Aswan granite reserved for Khafre's lower courses and part of Menkaure's pyramid.

Together, these monuments exemplify the geometric precision and advanced engineering of ancient Egyptian architecture.

METHODOLOGY

We analysed three GeoEye-1 images of the northern Egyptian desert, in the area surrounding the Giza Plateau. The GeoEye-1 VHR satellite simultaneously acquired panchromatic (PAN) and multispectral (MS) images, with a nadir Ground Sampling Distance (GSD) of 0.41 m and 1.65 m, respectively. Although acquired at 0.41 m resolution, the images distributed to commercial users were resampled to 0.5 m due to licensing restrictions with NOAA (GeoEye 2011). The MS bands were pansharpened to create 0.5 m colour images by fusing PAN and MS data. Both sensors provide 11-bit radiometric resolution (2,048 gray levels).

The GeoEye-1 data used for this study and their characteristics are listed in Tables 1 and 2. All three scenes were sorted with the panchromatic and multispectral bands separated, and after atmospheric correction

we performed resolution enhancement using the Gram-Schmidt Spectral Sharpening method (as implemented in the *ENVI* software).

RESULTS

Surroundings of the Giza Plateau

In November 2007, a field inspection was carried out in the area west of the Giza Plateau (Fig. 7, square A of Fig. 1) with the aim of verifying new hypotheses and interpretations proposed by Egyptologists.

This area lies west of the three pyramids, on the stratified nummulitic limestone formation known as Mokattam (Eocene), and has so far received little archaeological attention. It is situated at a higher elevation than the rest of the plateau, about 105 m above the Nile. Based on altimetry (Fig. 8), this western sector is hereafter referred to as the Third Level (Baratono 2004, 2008). The First Level therefore corresponds to the area of the Sphinx, about 15 m above the Nile, while the Second Level is occupied by the three pyramids at approximately 60 m.

Our investigation focused on the Third Level, where we documented traces suggesting the presence of a previously unknown quarry, in addition to the known ones indicated as A, B, and C in Fig. 8.

A photographic survey of the Third Level (Fig. 9a) highlights the difference in elevation compared to the pyramid plateau, a distinction further confirmed by the Digital Elevation Model (DEM) shown in Fig. 9b. The DEM illustrates the slope descending eastward from the Third Level (bottom) towards the pyramids (top, about 850 m away, Second Level), and further towards the Sphinx (First Level).

Fig. 9 - a) Photograph showing the elevation difference between the Third Level and the pyramid plateau (photo by D. Baratono); b) Digital Elevation Model of the Giza Plateau.

During the inspection, two subareas were identified on the Third Level containing numerous microlithic artefacts in chipped flint, including flaking tools or choppers. Retouched over their entire surface, these finds show similarities with lithic industries known from

Fig. 10 - Lithic artefacts found on the Third Level: amygdaloid tool, nucleus, flint blade from knapping, and a rounded quartzite with engraved motifs (photo by D. Baratono).

Fig. 11 - Ground traces indicating the existence of a quarry on the inspected site (photo by D. Baratono).

Fig. 12 - Rectangular depression at the western end of the Third Level, outlined in red (photo by D. Baratono).

North Africa (e.g. Capsian Neolithic), although a precise cultural attribution cannot be made without further analysis; they include amygdaloid tools, nuclei, blades, and points (Fig. 10). These sub-areas may therefore have functioned as microlithic stone-production zones, seemingly connected to the pyramid complex rather than to the surrounding landscape.

Additional ground traces observed on site (Fig. 11) further support the presence of quarrying activity. This evidence suggests the existence of another quarry besides those already documented to the south-east and north-west (points A, B, C in Fig. 8). These quarries likely supplied material for the massive core filling of the pyramids.

The evidence therefore suggests that the Third Level may have constituted an extraction and supply area from which construction material for the pyramids was obtained and transported.

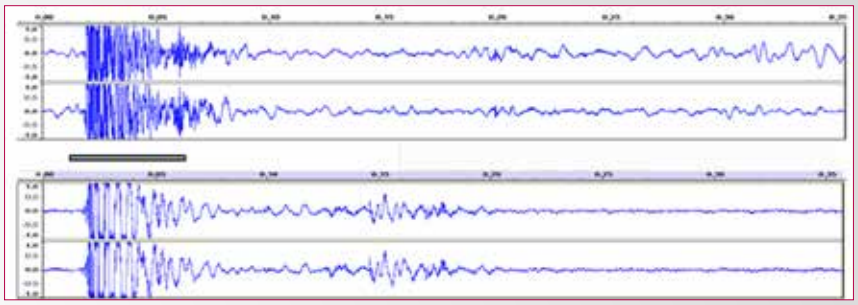

Fig. 13A - Acoustic signals recorded: upper, compact ground; lower, depression.

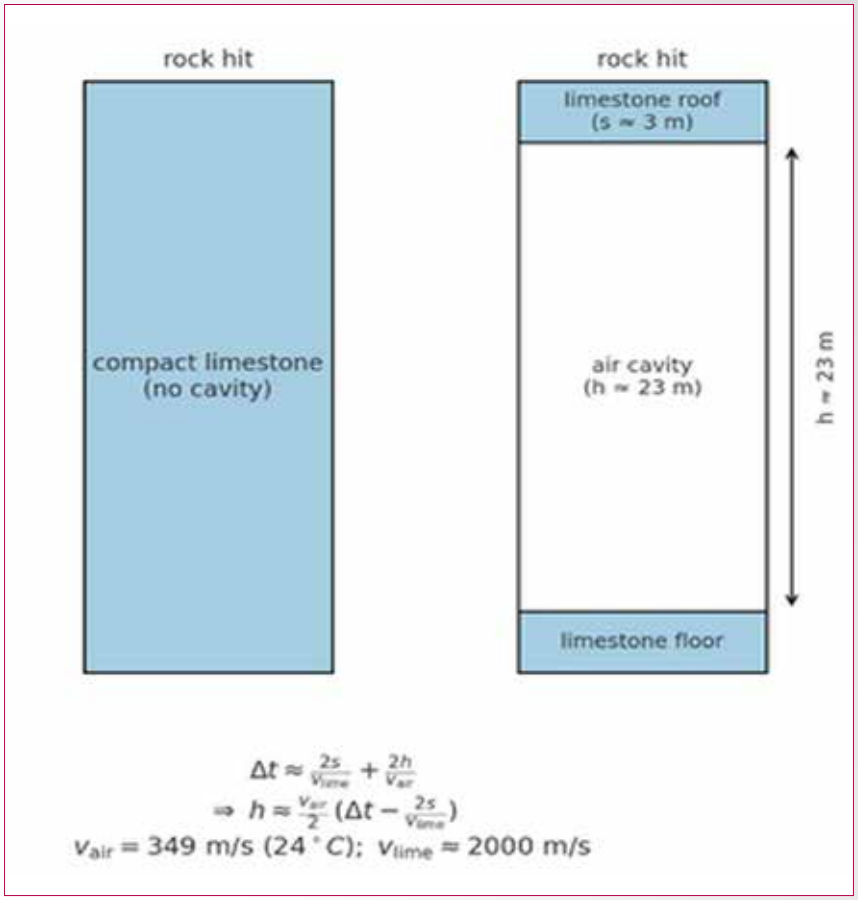

Fig. 13B - Acoustic analysis of the subsoil: schematic representation of the method used to infer the depth of the cavity.

Rectangular depression

Toward the natural end of the Third Level, much further west, just to the left of the heliport (H in Fig. 7), our on-site inspection revealed traces of a rectangular depression about the size of a football field (Fig. 12).

This structure is symmetrically aligned with the eastern site housing the Sphinx, from which it is almost equidistant.

A particularly noteworthy feature is that the area beneath the depression appears to be hollow. This was confirmed through acoustic testing, performed by striking the ground both outside and within the depression. The signals recorded with a camera placed at 1.5 m height (ambient temperature ≈ 24 °C) showed distinct differences (see Fig. 13a). Over compact ground the waveform was rapidly damped, with no late arrivals, whereas over the depression a delayed low-frequency wavetrain appeared. Spectral analysis highlights this contrast: the compact ground produced a short high-frequency packet, while above the hollow the spectrum shifted to lower frequencies, an effect consistent with a rigid roof over an underground void that acts as a high-frequency filter.

From the change in frequency content immediately after the first arrival (≈0.02 s), the thickness of the limestone roof can be estimated at about 2.5-3.5 m. More importantly, a distinct secondary arrival at ≈0.15 s corresponds to the echo from the cavity floor. The travel-time difference ($\Delta t \approx 0.13$ s) can be modelled as two crossings of the roof in limestone ($v_{lime} \approx 2000$ m/s) plus a two-way path through the air-filled chamber ($v_{air} = 349$ m/s at 24 °C). Applying the relation:

$$\Delta t \approx \frac{2s}{v_{lime}} + \frac{2h}{v_{air}}$$

$$\Rightarrow h \approx \frac{v_{air}}{2}\left(\Delta t - \frac{2s}{v_{lime}}\right)$$

The contribution of the limestone roof is small: with $s \approx 3$ m and $v_{lime} \approx 2000$ m/s, the term $2s/v_{lime} \approx 0.003$ s, negligible compared to $\Delta t \approx 0.13$ s. Therefore, the depth of the cavity floor is estimated at $h \approx 23$ m beneath a roof of about 3 m of compact limestone (see Fig. 13b), with an uncertainty of several meters due to assumptions on wave velocity and local geology.

It is not uncommon to find underground structures in this archaeological area, as shown by recent discoveries (Sato et al. 2024).

Boats

Along the southern side of Khufu's Pyramid (Fig. 14*), five boat pits were discovered, two of which still contained disassembled ritual boats*. One, likely used for Khufu's funeral, has been reassembled in an on-site museum.

A few kilometres west of the Giza Plateau, in box B of Fig. 1, satellite image analysis revealed 56 traces over ~11 km^2,

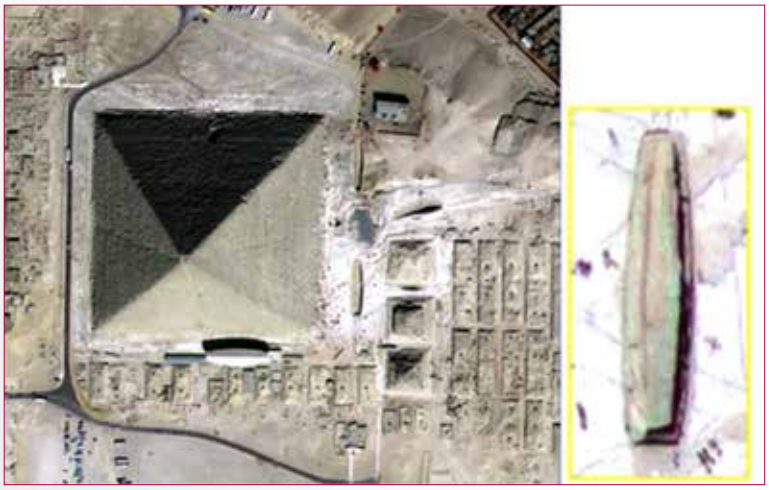

Fig. 14 - Pyramid of Khufu and the discovered solar boat (yellow square), to be compared with a sand pattern southwest of the Giza Plateau in the GeoEye-1 image.

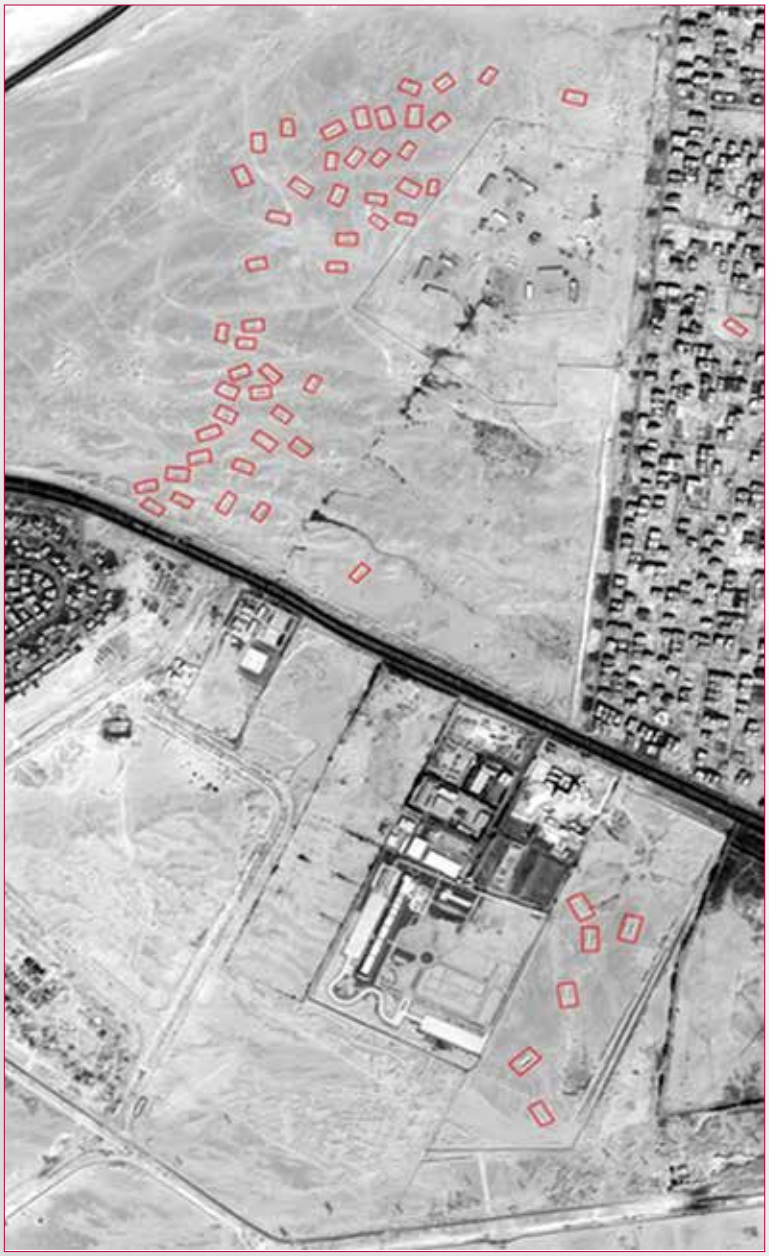

Fig. 15 - Portion of the GeoEye-1 image southwest of Giza showing 56 traces (red rectangles) comparable in size to the solar boat pit near the Pyramid of Khufu.

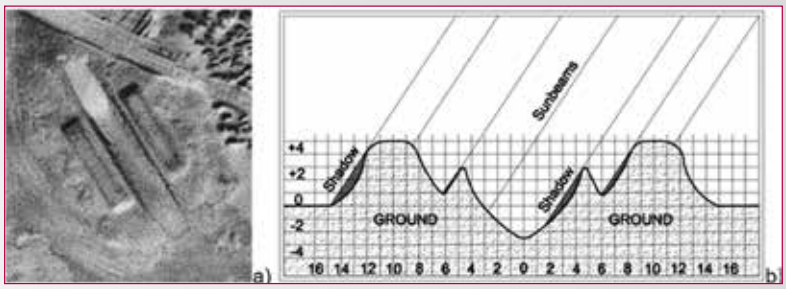

Fig. 16. a) Sand pattern comparable in size and shape to the solar boat pit near the Pyramid of Khufu; b) Cross-section profile (m) inferred from shadow analysis.

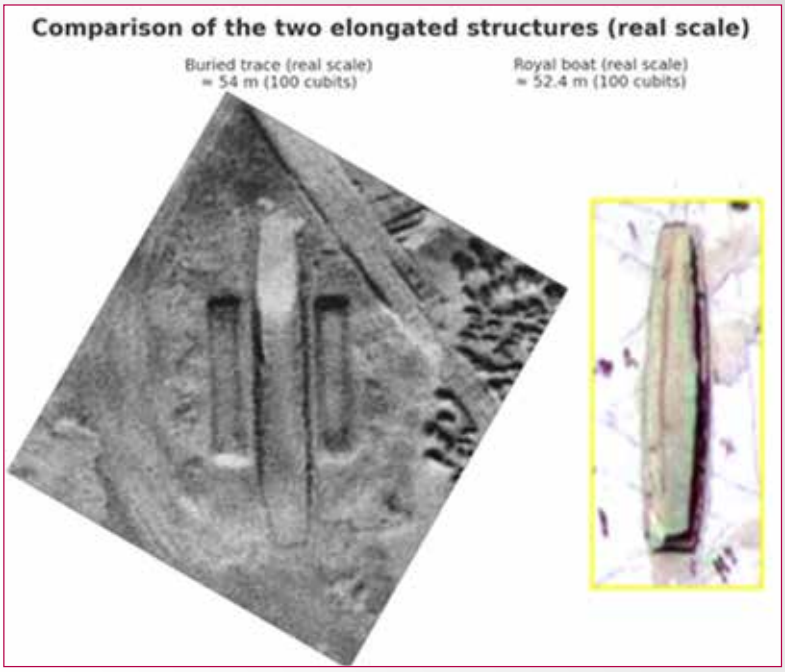

Fig. 17 - Side-by-side comparison of the buried trace and the Royal Boat, displayed at the same scale (lengths in m and Royal Cubits).

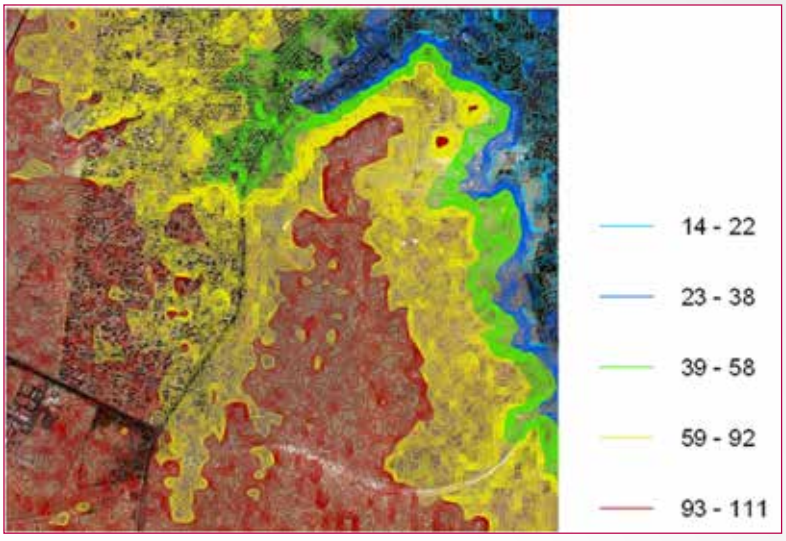

Fig. 18 - Topographic map overlaid on the Giza site plan; colours indicate altitude ranges (m).

shown in Fig. 15 and shaped similarly to the boat pit in Fig. 14. Their morphology is compatible with possible buried boats or storage structures west of Giza, although excavation is required to confirm this interpretation.

To reconstruct the cross-sectional profile of the sand features (Fig. 16a), we used data in Table 1. The image of 5 November 2010 ($\alpha = 41.7^{\circ}$) provided the clearest shadows; by elementary trigonometry the ridge height is

$$h = L \tan(\alpha)$$

where L is shadow length and α solar elevation. The section in Fig. 16a yields the distribution in Fig. 16b, highlighting a central elongated relief, comparable in size/shape to Khufu's boat pit, flanked by rectangular forms.

The traces (Fig. 15) split into two size classes: 50 traces in the northern half of area B measure 39 ± 3 m, and 6 traces in the southern half measure 54 ± 2 m, the latter dimensions are consistent with boats of Khufu's reign (Palermo Stone ≈ 100 Royal Cubits = 52.36 m; Fig. 17).

Thus, one group corresponds to ~75 Royal Cubits (39.27 m) and the other to ~100 Royal Cubits. Comparable finds exist (e.g., a wooden solar boat of 18 m = 34 Royal Cubits discovered at Saqqara in 2016 (Il Fatto Storico 2016). Their morphology and dimensions are consistent with possible buried boats, potentially indicating a shipyard or storage area west of Giza.

This hypothesis is strengthened by topographic/geomorphological analysis (Fig. 18) and by the 3D surface model (Fig. 19), which indicates a probable ancient waterway active during Nile floods that may have connected the depot to the plateau.

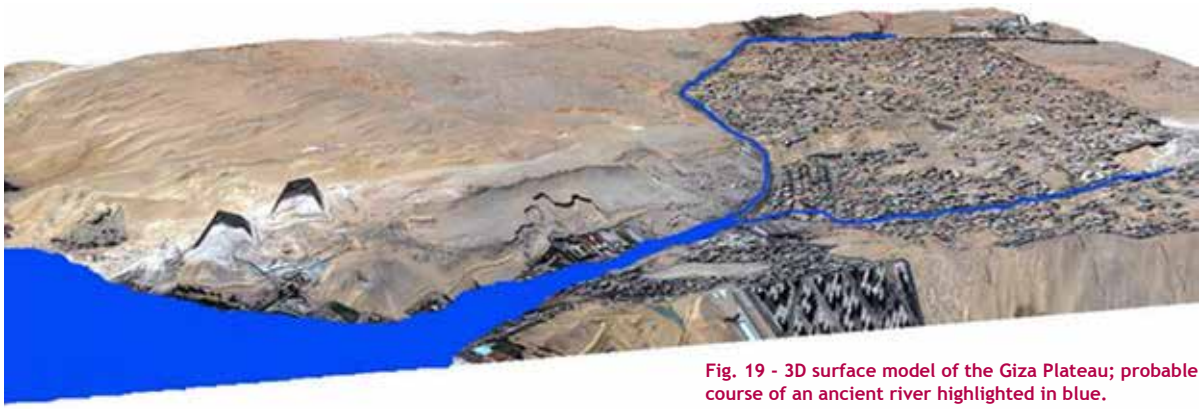

Fig. 19 - 3D surface model of the Giza Plateau; probable course of an ancient river highlighted in blue.

Studies have indicated that the Giza Plateau was bordered by channels filled during seasonal floods, enabling navigation (Fig. 20). Historical sources also record canals deliberately dug by pharaohs: Diodorus Siculus (1933) notes locks and dams; Goyon (1977) views the canal network as a *conditio sine qua non* for pyramid construction; the Palermo Stone records large boats, further examined by Wilkinson (2000). Archaeological reconstructions suggest a harbour near Khafre's valley temple, a raised platform with parapet (~9 m wide), drainage holes, and a sloping beach, likely used for docking/storage and possibly active since the Third Dynasty, serving also neighbouring fields (Abu Rawash, Abusir, Abu Gorab, Saqqara, Dahshur).

Without direct excavation or field survey no definitive conclusion can be drawn; nonetheless, the convergence of satellite evidence, dimensional analysis, topography, and historical records supports the interpretation of these anomalies as buried boats or harbour installations.

Ancient Necropolis

Area C, shown in Fig. 1 and enlarged in Fig. 21a, covers approximately 0.5 km² and contains 975 rectangular structures, each measuring about 27 m² (6.5 m × 4.2 m, or 12.5 × 8 Royal Cubits, equivalent to 100 square Royal Cubits). The arrangement of these structures is suggestive of an ancient workers' village or a necropolis.

Ancient Port and Old Fort

Visual inspection of the GeoEye images for Area D (Fig. 1) revealed intriguing traces, enlarged in Figs. 22a and 22b.

The sand-covered structure in Fig. 22a, covering about 0.12 km², resembles the layout of a buried ancient building. It features a central corridor measuring 225 m in length and 10 m in width, oriented NW-SE, with perpendicular corridors on either side terminating in small rooms.

In Fig. 22b, covering around 0.1

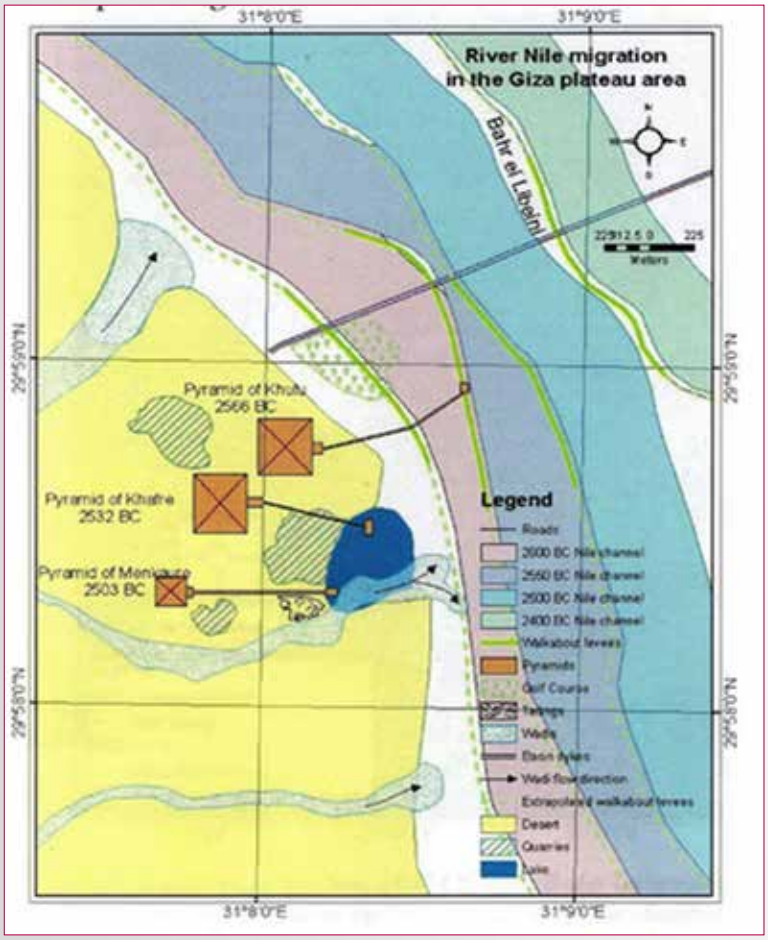

Fig. 20 - Waterways near the Giza Plateau: map of the Nile's westward shift at Giza (source: Lutley & Bunbury 2008).

km², is a structure composed of 24 U-shaped traces, each 29 Royal Cubits (15 m) long and 16 Royal Cubits (8.5 m) wide, arranged in a pattern resembling the towers of an ancient fortress.

These traces are inscribed within a circle measuring 500 Royal Cubits (262 m) in diameter (Fig. 23a). Fig. 23b shows the sand profile of a single structure, derived using the same shadow-analysis method described earlier.

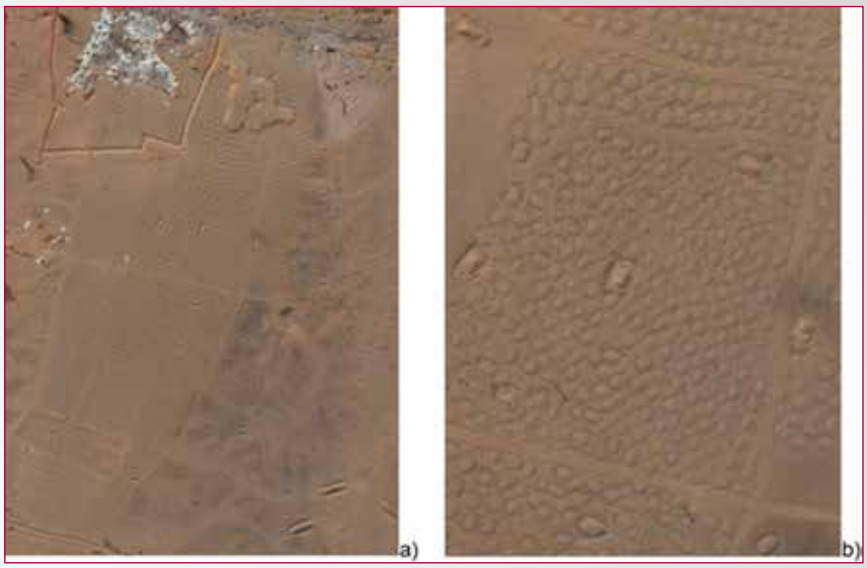

Fig. 21 - a) Area C (see Fig. 1): 975 rectangular traces across ~0.5 km²; b) Enlarged portion.

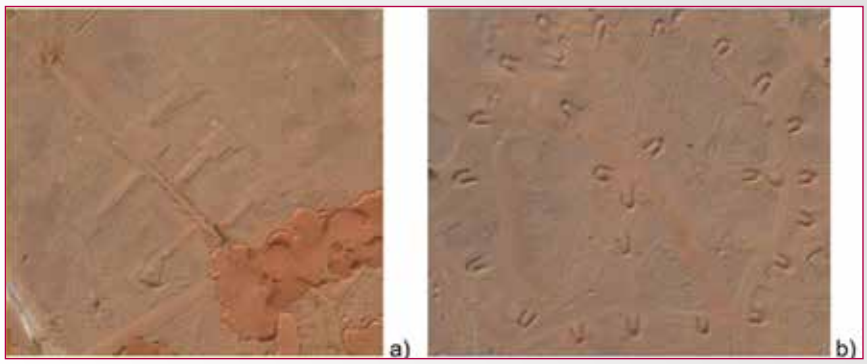

Fig. 22 - a) Traces resembling an ancient port; b) U-shaped traces arranged like the towers of a fort.

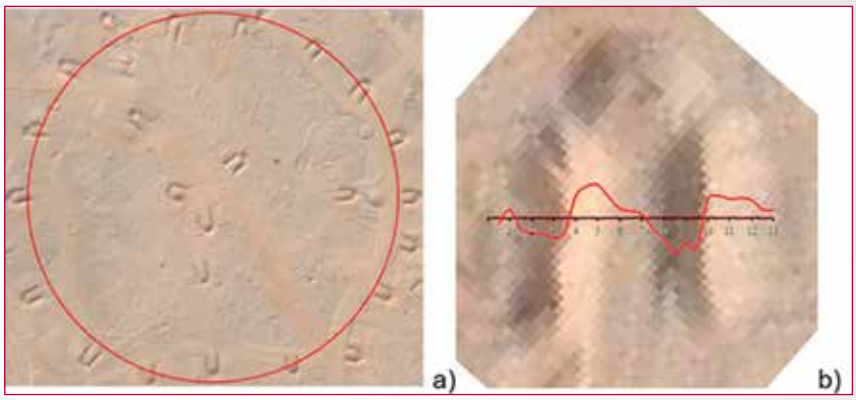

Fig. 23 - a) U-shaped traces inscribed in a circle of ~500 Royal Cubits (262 m); b) Sand profile of a single structure derived from shadow analysis.

CONCLUSIONS

High-resolution satellite imagery analysis is an effective approach for detecting structures buried beneath sand, particularly in archaeologically significant areas. At the Giza site, this approach revealed numerous traces of potential interest. Combined with on-site surveys and subsequent analyses, these observations have enabled the formulation of preliminary hypotheses on what might lie underground, to be validated through dedicated archaeological surveys. Analysis of solar angles and satellite viewing geometry further allows the reconstruction of sand profiles that conceal such structures by interpreting the shadows they cast. Ultimately, direct fieldwork, particularly excavation, remains essential to determine the true nature of each anomaly. Nevertheless, the methodology enables rapid mapping and supports targeted archaeological research.

Bibliografia

Baratono, D. (2004) *Le abbazie ed il segreto delle piramidi. L'Esagramma, ovvero le straordinarie geometrie dell'acqua*. Genova: ECIG. ISBN 8875459983.

Baratono, D. (2008) Le tre piramidi di Giza furono costruite dall'alto? *ArcheoMisteri* 38 (marzo/aprile), Firenze. *(included for contextual completeness)*.

Diodorus Siculus (1933) *Bibliotheca historica*, Book I. Transl. by C.H. Oldfather. Cambridge, MA: Harvard University Press.

GeoEye (2011) *GeoEye-1 Satellite Imagery Product Guide*. [online] Available at: [link not available] (Accessed: 20.08.2025).

Goyon, J.C. (1977) *Les travaux de Chéops au temple d'Isis, dame du pyramidion*. Le Caire: Institut Français d'Archéologie Orientale.

Il Fatto Storico (2016) Barca solare scoperta a Saqqara. [online] Available at: https://ilfattostorico.com/2011/07/01/la-nuova-barca-solare-del-faraone/ (Accessed: 20.08.2025). (included for contextual completeness).

ITT Visual Information Solutions (2009) *ENVI User's Guide*. Boulder, Colorado: ITT Visual Information Solutions, pp. 407–410.

Jahjah, M. & Ulivieri, C. (2010) Automatic archaeological feature extraction from satellite VHR images. *Acta Astronautica* 66, 1302–1310.

Lasaponara, R. & Masini, N. (2007) Detection of archaeological crop marks by using satellite QuickBird multispectral imagery. *Journal of Archaeological Science* 34, 214–221.

Lutley, K. & Bunbury, J.M. (2008) The Nile on the move. *Egyptian Archaeology* 32, 3–5.

Masini, N. & Lasaponara, R. (2007) Investigating the spectral capability of QuickBird data to detect archaeological remains buried under vegetated and not vegetated areas. *Journal of Cultural Heritage* 8, 53–60.

Rowlands, A. & Sarris, A. (2007) Detection of exposed and subsurface archaeological remains using multi-sensor remote sensing. *Journal of Archaeological Science* 34, 795–803.

Sato, M., Saito, R., Abbas, A.M., Mesbah, H., Taha, A., Gaweish, W.R., Aldeep, M., Kurokouchi, H., Takahashi, K., El-Qady, G. & Yoshimura, S. (2024) GPR and ERT exploration in the Western Cemetery in Giza, Egypt. *Archaeological Prospection*. https://doi.org/10.1002/arp.1940

Traviglia, A. & Cottica, D. (2011) Remote sensing applications and archaeological research in the Northern Lagoon of Venice: the case of the lost settlement of Constanciacus. *Journal of Archaeological Science* 38, 2040–2050.

Trier, Ø.D., Larsen, S.Ø. & Solberg, R. (2009) Automatic detection of circular structures in high-resolution satellite images of agricultural land. *Archaeological Prospection* 16, 1–15.

Wilkinson, T.A.H. (2000) *Royal Annals of Ancient Egypt: The Palermo Stone and its associated fragments*. London: Kegan Paul International.

Abstract

A methodology for analysing very high-resolution (VHR) satellite images was developed to detect buried structures in arid regions using optical and infrared bands. Applied to the desert around the Giza Plateau, it revealed four sand-covered areas of interest. West of the pyramids, evidence of quarrying activities and an underground chamber was identified. Shadow analysis suggested buried vessels, possibly a depot linked to pyramid construction, while 3D topography indicated a probable ancient waterway. Additional features, including tombs, architectural remains, and other buried structures, were also detected and described.

Parole Chiave

Surveying archaeological sites in arid areas; satellite remote sensing; high-resolution imagery; landscape archaeology; 3D topographic analysis

Autore

Paolo Trivero
paolo.trivero@uniupo.it
Former Full Professor of Physics at the University of Eastern Piedmont (UPO), now retired.

Diego Baratono
diego.baratono@yahoo.it
Independent researcher

Maria Borasi
maria.borasi@libero.it
Former research fellow at the University of Eastern Piedmont (UPO), now independent researcher.

Marco Cavagnero
cavagnero.m@gmail.com
Former research fellow at the University of Eastern Piedmont (UPO), now independent researcher.